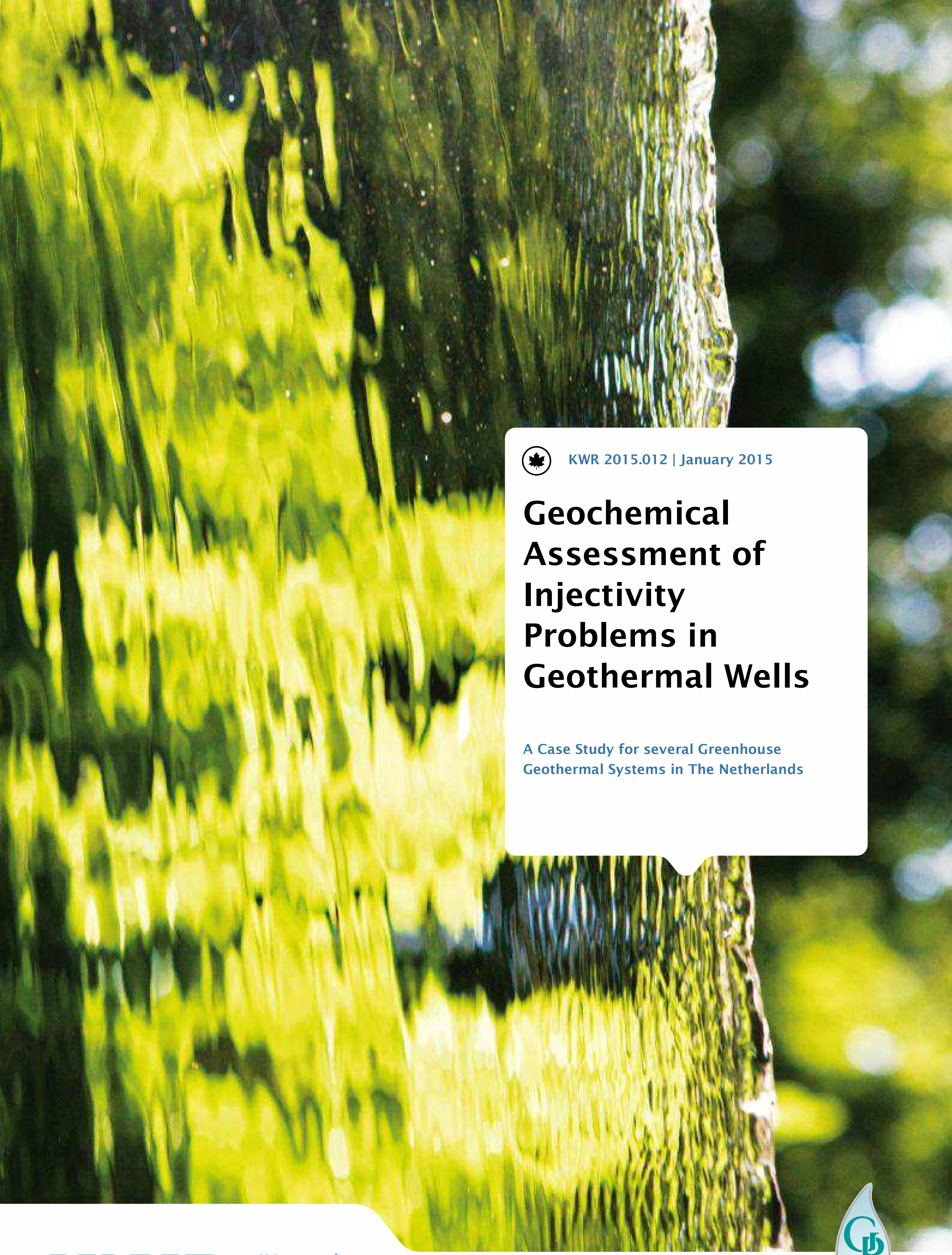

KWR 2015.012 | January 2015

Geochemical Assessment of Injectivity Problems in Geothermal Wells

A Case Study for several Greenhouse Geothermal Systems in The Netherlands

KWR Watercycle Research Institute

Geochemical Assessment of Injectivity Problems in Geothermal Wells

A Case Study for several Greenhouse Geothermal Systems in The Netherlands

KWR 2015.012 | January 2015

Project number
A309539

Project manager
Klaasjan Raat

Client
Ammerlaan TGI

Quality Assurance
Prof. Dr. Pieter Stuyfzand

Author(s)
Dr. Niels Hartog

Sent to
Leon Ammerlaan

Year of publishing
2015

More information
Dr. Niels Hartog
T
E niels.hartog@kwrwater.nl

PO Box 1072
3430 BB Nieuwegein
The Netherlands

T +31 (0)30 60 69 511
F +31 (0)30 60 61 165
E info@kwrwater.nl
I www.kwrwater.nl

Watercycle
Research
Institute

Summary

The horticultural sector is making increasing use of geothermal heat as a renewable substitute for the burning of natural gas. However, so far many of the completed geothermal systems in the Netherlands do not function as planned. After heat extraction, the water is reinjected into the reservoir. A frequent problem with this is the poor injectivity of the injection wells.

The causes of injectivity problems at several geothermal systems used by the greenhouse industry were investigated by analysing the geochemical aspects and processes involved. This study focuses on the causes of the poor injectivity. Within this research GPC (France) focussed on the measurements of bubble point pressure and suspended particle size distributions, while KWR Watercycle Research Institute focussed on the (geo)chemical processes that occur in the geothermal systems. KWR's research is reported here. Particular focus was on the precipitation of minerals, as mineral scaling was suspected to be a major contributor to the injectivity problems.

It is concluded that the main cause for accumulation of minerals on filters and as scaling is the degassing of CO2 during the rise in the production well and in subsequent parts of the geothermal system. The CO2 degassing results from the drop in the gas pressure at reservoir depth (hydrostatic pressure) to the relatively low pressure at which the geothermal system at the surface is operated. The loss of CO2 results in subsequent precipitation of carbonate minerals.

Depending on the chemical composition of the geothermal water in the reservoir, Ca-rich, Fe-rich or Pb-rich carbonates were preferentially precipitated, as was confirmed by analysis of filter and scaling accumulates from various systems.

Since degassing of CO2 pressure acts as the main driver for the carbonate precipitation observed, CO2 pressure control also provides a solution. Luckily, since CO2 appears to only represent a relatively small fraction of the total gas pressure in the geothermal reservoirs studied, only a limited level of CO2-dosing is required to prevent or re-dissolve carbonate precipitates. The required partial CO2 pressure seems well achievable within the operational pressures currently maintained in the geothermal systems. For sites with lead carbonate precipitation, an increased CO2 pressure is required to compensate for the decrease of lead carbonate solubility with lower temperatures.

-

Contents

1 Introduction

1.1 Background

The horticultural sector is making increasing use of geothermal heat as a renewable substitute for the burning of natural gas. However, so far many of the completed geothermal systems in the Netherlands do not function as planned. After heat extraction, the water is reinjected into the reservoir. A frequent problem with this is the poor injectivity of the injection wells.

This study focuses on the causes of the poor injectivity. Within this research GPC (France) focussed on the doublet performance assessment, while KWR Watercycle Research Institute focussed on the (geo)chemical processes that occur in the geothermal systems. The results of the doublet performance assesment are presented in GPC (2014). Here, the geochemical part of the study is presented. Particular focus was on the precipitation of minerals, as mineral scaling was suspected to be a major contributor to the injectivity problems.

1.2 Sites studied

Table 1: Geothermal systems for which the water and scale composition were analysed in this study (x). Additional geothermal sites for which production water composition was compiled by (Wasch, 2014) are also listed.

Site#	Owner	Code	Location	Water	Scaling
1	Ammerlaan	AML	Pijnacker	x	x
2	Van den Bosch	VDB1	Berkel	x	
3	Van den Bosch	VDB2	Bleiswijk	x	
4	Gebr. Duijvestijn	DVS	Pijnacker	x	
5	Greenwell	GW	Honselersdijk	x	x
6	Wijnen	WN-01 WN-03	Californië (Grubbevorst)	x x	
7	Aardwarmtecluster KKP	ACK	Koekoekspolder	TNO	x
8	ECW	ECW	Middenmeer	TNO	
9	Floricultura	FC	Heemskerk	TNO	

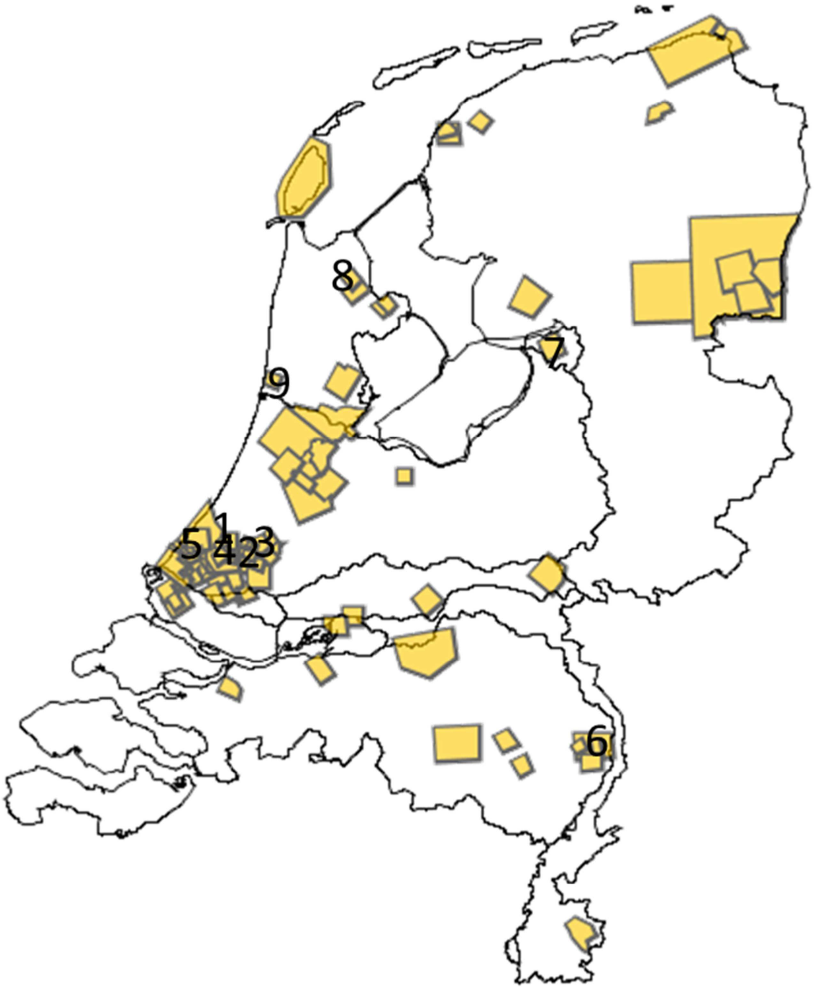

Figure 1: Locations of the 7 geothermal systems studied (1-7, Table 1), with indication of the areas currently having a geothermal permit in The Netherlands (thermogis.nl). The locations of 3 additional sites (7, 8 and 9) for which produced water composition was included as reference are also shown.

2 Methods

2.1 Water sampling and field measurements

Objective was to sample at least the produced and injected water, to allow detection of chemical changes that could be indicative of geochemical processes. Due to operational factors this was not possible for all sites. For other sites, additional samples, in between degasser and the heat exchange unit could be taken. KWR conducted the water sampling and prepared the samples in the field for analysis. PJ Milieu conducted the gas sampling. Sampling for dissolved gas was performed under pressure using stainless steel cylinders, compatible with the connectors used to extract the gas for analysis, to minimize the risk of gas losses and atmospheric contamination.

Figure 2: Stainless steel cylinder used for gas sampling.

Parameters determined in the field were temperature, pH and electrical conductivity.

2.2 Chemical Analysis

On the same day of sampling, the samples taken were transfered to the various laboratories. The storage period was kept to a minimum and analysis was performed within a few days.

2.2.1 Water analyses

Water compositions was determined by wet chemical analysis (Table 2). The cations and trace elements were analyzed with ICP-MS after total destruction using HNO_3 without and after filtration (0.45µm). Anions were analyzed using ion chromatography (HCO_3, Cl, SO_4, F). Separate analyses were performed for NH_4, PO_4, sulfide, and silica content. Microbiological analyses were performed for microbial activity and ATP biomass analysis.

Table 2: Water analyses performed on the geothermal systems studied. The water type labels P and I indicated production and injection wells respectively. For water type D, the water between the degasser and the heat exchanger was sampled. For sites 7-9 the composition of production water was taken from the compiled data by TNO (Wasch, 2014)

Site#	Owner	Code	Location	Water Type
1	Ammerlaan	AML	Pijnacker	P, D, I
2	Van den Bosch	VDB1	Berkel	P,I
3	Van den Bosch	VDB2	Bleiswijk	P,I
4	Gebr. Duijvestijn	DVS	Pijnacker	P,I
5	Greenwell	GW	Honselersdijk	P,I
6	Wijnen	WN-01 WN-03	Californië (Grubbevorst)	P P
7	Aardwarmtecluster KKP	ACK1 ACK2	Koekoekspolder	P(TNO) P(TNO)
8	ECW	ECW	Middenmeer	P(TNO)
9	Floricultura	FC	Heemskerk	P(TNO)

2.2.2 Gas analyses

The cylinders containing the pressured samples of production and injection water (Table 3) were processed by ISOLAB BV by releasing (flashing) a small part of the total gas pressure into a small headspace volume, followed by GC analysis using helium as carrier gas. Analysis was performed in triplicate. The gas composition was determined by analyzing for the following gas components: N2, CO2, H2S, Methane (C1, CH4), Ethene, C2 (Ethane), Propene, C3 (propane), iC4, nC4 (i- and n-butane), neo-C5, iC5, nC5 (pentane) and C6+ (hexane and longer carbon chains). For the injection waters at sites 1 and 4, repeat analysis was performed with argon as carrier gas, to verify the presence of helium in the extracted gas.

Table 3: Sites for which the gas composition of the produced (P) and injected (I) water was determined.

Site#	Code	Location	Water Type	Comment
1	AML	Pijnacker	P,I	
3	VDB2	Bleiswijk	P,I	
4	DVS	Pijnacker	P,I	
5	GW	Honselersdijk	P,I	
6	WN	Californië (Grubbevorst)	P(-01) P(-03)	Insufficient gas for complete analysis

-

2.2.3 Scale analysis

Samples from material accumulated on filters or as scaling were collected from three sites (Table 4). Analysis was performed after total destruction using HNO3, followed by the same inorganic elemental analysis as described for the water samples (paragraph 2.2.1).

Table 4: Geothermal systems from which the composition of accumulations as scalant and/or in the filter was determined.

Site#	Code	Location	Type	Sample Description
1	AML	Pijnacker	Scalant	Brown chunks on flange window
			Filter	Scale on stainless steel filter
5	GW	Honselersdijk	Filter	Filter with trapped particles
7	ACK	Koekoekspolder	Scalant	Slurry taken from the bottom

3 Results and Discussion

3.1 Chemistry of geothermal waters

The scaling potential during the extraction of water from deep geothermal reservoirs depends foremost on the composition of the geothermal water itself. With the high dissolved contents that characterize these waters, also the potential for mineral precipitation increases. The extent however to which this might occur, depends on the type and extent of physico-chemical changes that occur with respect to the reservoir conditions from which the geothermal water was pumped. The most important changes that occur during the processing of geothermal water are the:

- temperature decrease during heat extraction (main purpose)
- total pressure decrease, as the geothermal water is pumped from great depths with high hydrostatic pressures (e.g. >200bar at 2000m depth)

Here, we first focus on the composition of the various geothermal waters analyzed, as it is the first factor that affects which and to what extent mineral precipitation might be induced by changes during the process of geothermal heat extraction. Secondly, we address how water quality changes from production to injection, to address any noticeable changes that could indicate the occurrence of mineral precipitation or any other geochemical process that could lead to injectivity problems. Finally, we relate the various compositions of geothermal waters to the composition of accumulations for several of the geothermal systems studied.

3.1.1 Salinity

Sodium and chloride are the main constituents for all geothermal waters studied and their correlations are well established. The ratio between chloride and sodium indicates that their high salinities are mainly the result from the evapo-concentration or hyperfiltration of seawater. Only site 1 (AML) is shifted closer to the ratio expected for halite (NaCl) dissolution. For all sites however, sodium and chloride concentrations are well below (>2x) those expected for halite equilibrium, even when cooled to a temperature of 30°C. Halite precipitation is therefore not expected to occur in any of the geothermal systems.

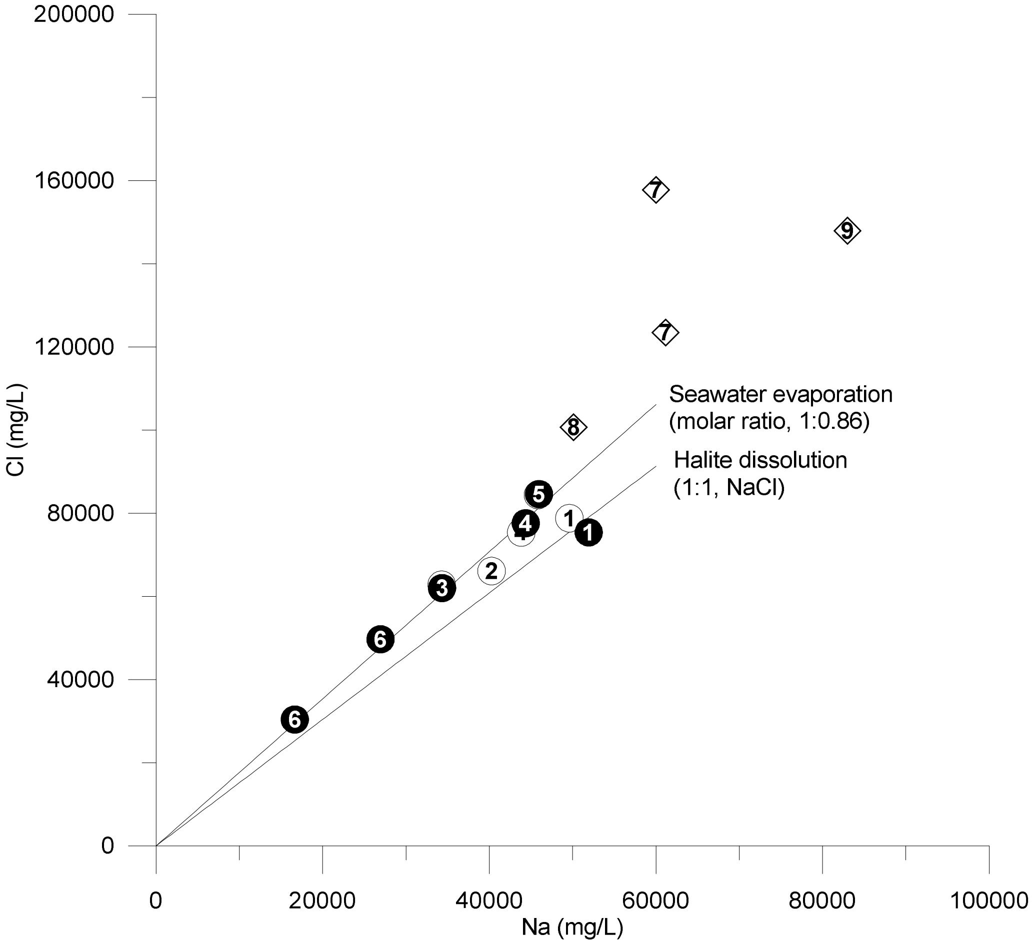

Figure 3: Sodium (Na) versus chloride (Cl) concentrations in the produced water (black circles) for the studied sites. Numbers refer to the sites listed in Table 1. The diamonds indicate the compositions from the compilation by (Wasch, 2014).

3.1.2 Gas compositions

The total amount and composition of gas dissolved in the geothermal waters are important aspects when pressure changes occur in the geothermal system. In the reservoir, the maximum amount of gas that can be dissolved is related to the total pressure in the reservoir. In the absence of over- or under pressure, this total pressure is equal to the hydrostatic pressure exerted by the height of the overlying water column. Therefore, with increasing depths, the hydrostatic pressure increases and for reservoir depths over 2km, hydrostatic pressures and thus maximum dissolved gas pressures are over 200atm. Whether or not the dissolved gas pressure equals the hydrostatic gas pressure depends on whether or not sufficient gas is available. In the presence of known free gas occurrences, this is surely the case. Typically, the above-ground geothermal system is operating under pressures that are at least multiple times lower (e.g. 15 atm) than the hydrostatic pressure in the aquifer from which the geothermal water is produced. Therefore it is expected that degassing occurs as the produced geothermal water is pumped upward along the pressure gradient. This is in keeping with the observations by GPC for the studied sites that the pressure in the production well had already dropped below the bubbling point (GPC, 2014), i.e. the gas pressure already exceeded the hydrostatic pressure in the upper part of the well and a free gas phase had already formed.

Degassing itself can cause clogging and injectivity problems, as reduction in water permeability occurs in the presence of free gas. The use of a degasser, will aid the prevention of gas clogging by removing the amount of free gas that is produced by the time the produced water reaches the surface operation. However, in the formation and removal of free gas the potential for the precipitation of carbonate minerals is induced, according to the following reaction in case of the precipitation of calcite (CaCO3):

$Ca^{2+} + 2\ HCO3^{-} = CaCO_3(s) + CO_2(g) + H2O(l)$

where HCO3- is measured as alkalinity (or acid buffering capacity) and the subscripts s, g and l refer to the formation of solid, gas and liquid phases.

The extent to which carbonate minerals precipitate therefore depends on the amount of CO2 removal during degassing, which in turn depends on the partial pressure of CO2 in the reservoir. This partial pressure is a function of the molar (~volumetric) fraction of CO2 in the gas and the total gas pressure in the reservoir.

Results of the analyses on the gas contained in the produced water (Figure 4), indicate that methane (CH4) is the major component (>85%) in the dissolved gas phase for sites 1, 3 and 4. For site 5 (GW) and particularly site 6 (WN) the methane fraction is lower at 75% and 25% respectively. For the methane rich samples, CO2 represents the second-largest fraction (few percent) of the remaining gasses present. Overall, these gas compositions fall well within the range of the majority of gas compositions measured during gas- and oil exploration (nlog.nl).

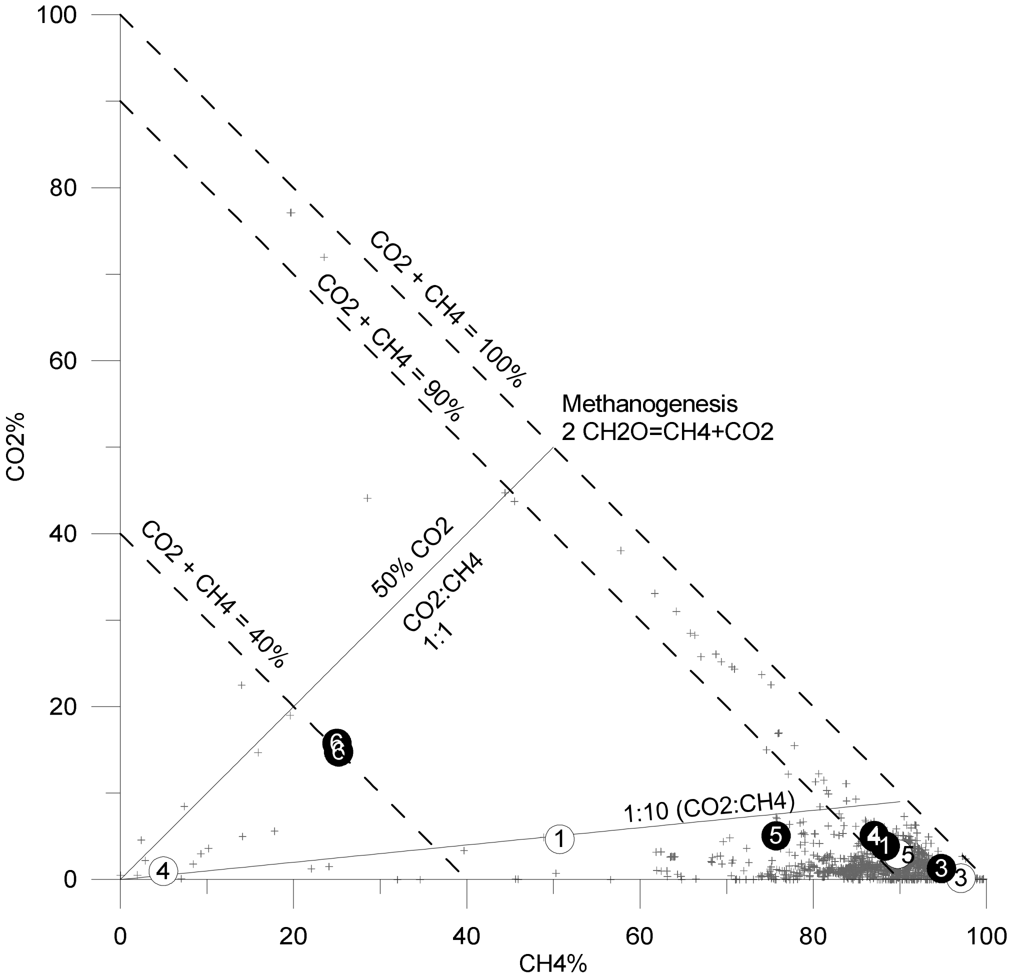

Figure 4: The relative proportions of methane (CH4) versus carbon dioxide (CO2) in the total amount of gas extracted from the geothermal waters. Numbers refer to the sites as listed in Table 1. Black circles refer to the compositions in the produced water, white circles refer to the composition in the injected water. For reference, the grey plusses indicate gas compositions measured for Dutch oil and gas production sites (nlog.nl).

The determined dissolved gas composition for the produced water at site 6 (WN) has a relatively low carbon dioxide and methane fraction. Due to the relatively low gas content in the produced water at site 6 (WN) location, the content of gases other than CO2 and CH4 could not be determined. However, in contrast with the produced water on the other sites, the near equal content for these two species would be indicative of a methanogenic contribution rather than a thermogenic origin of the methane. This is also supported by the relatively low ethane fraction (Figure 5). In contrast, the relatively high ethane fraction for particularly site 1 (AML) indicates the presence of a “wet gas” with oil related compounds.

Strikingly, the relative methane fractions were strongly reduced (Figure 4) in the injection water for site 1 (AML) and 4 (DVS), both sites that operate a degasser. For typical gas compositions, the predominant fractions besides methane and CO2 is nitrogen (N2). Nitrogen however, accounted only for 31% and 3.9% of the total gas composition. After switching the carrier gas of the GC to argon, it was verified that in addition to nitrogen, helium contributed to 22% and 88% of the gas phase. The strong increase in the percentage of helium in the injection water for these geothermal systems, is attributed to the relatively low gas pressure remaining in the water after degassing. Since helium has a very high Henry's constant, this results in preferential loss of helium from the sampled water when partitioning with the headspace during extraction. Therefore, for these two sites, it is expected that fractionation during gas sampling resulted in an overestimation of the most volatile gasses such as particularly helium. To a lesser extent, this is also reflected in the relative increase of methane compared to ethane in the injection waters for sites 1, 4 and 5 (Figure 5)

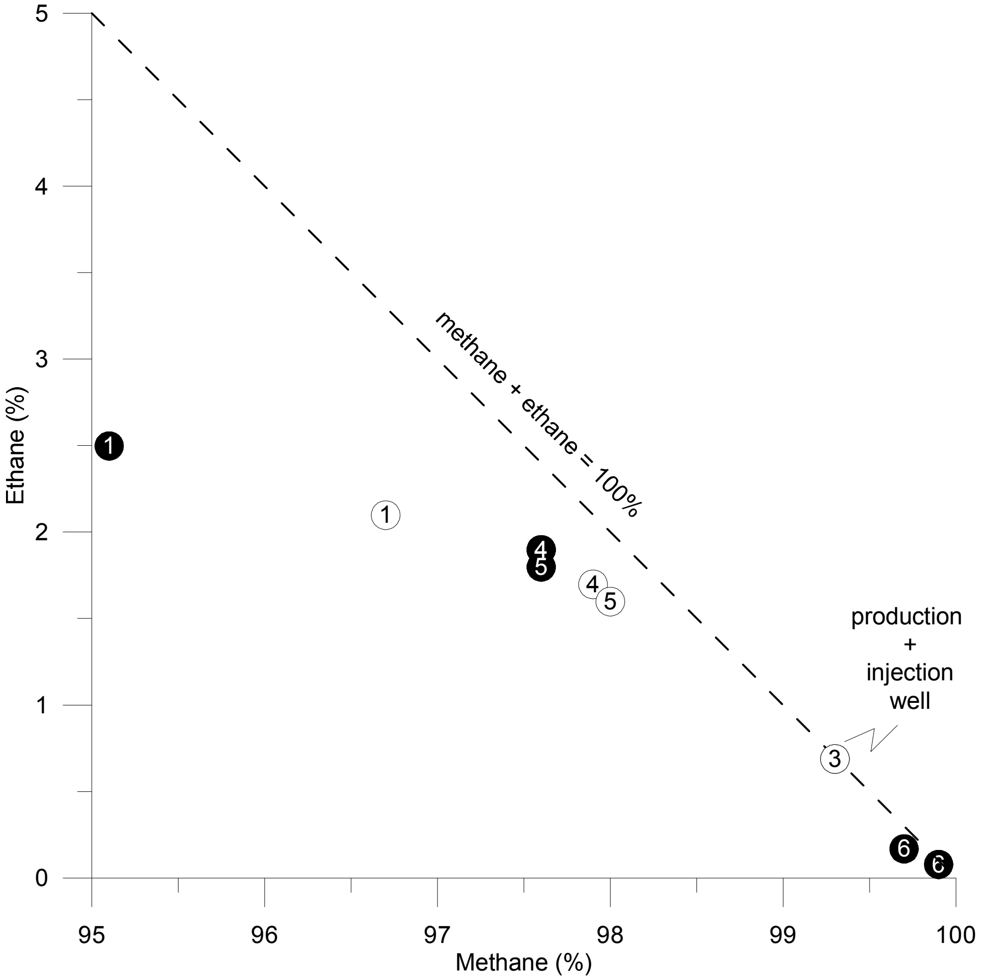

Figure 5: The relative proportions of methane (CH4) versus ethane as a fraction of the total organic components (C1-C6+) in the gas extracted from the geothermal waters. Numbers refer to the sites as listed in Table 1. Black circles refer to the compositions in the produced water, white circles refer to the composition in the injected water.

3.1.3 Carbonate-CO2 equilibria

The amount of carbonate that can precipitate due to CO2 degassing depends on the alkalinity and the concentration of available cations to form a carbonate phase. Unlike most common minerals, carbonates are more soluble with lower temperatures. This is illustrated when comparing the modelled calcite solubilities for different temperatures at identical CO2 pressures (Figure 6). Therefore, cooling would act to decrease the scaling potential induced by CO2 degassing. A noteworthy exception is however the lead mineral cerrusite, a carbonate ($PbCO_3$), the solubility of which does decrease with decreasing temperatures (http://thermoddem.brgm.fr).

The geothermal waters analysed are relatively rich in calcium compared to alkalinity, as are many other Dutch reservoirs as illustrated by the data from (Verweij, 2003). This means that stoichiometrically, there is sufficient calcium present to precipitate all alkalinity as calcite ($CaCO_3$). Since alkalinity is limiting the potential for calcite precipitation, site 6 (WN), with the highest alkalinity is the geothermal system with the highest calcite precipitation potential. However, the extent to which various carbonate minerals, or more likely, mixtures thereof, precipitate depends strongly on the rate with which they precipitate. This favours the precipitation of less soluble carbonates such as iron or lead carbonates, if sufficient concentrations of these cations are available for precipitation.

As shown by GPC (2014), CO_2 represents only a small fraction of the total gas pressure. However, for a hydrostatic pressure in the originating reservoir of 200atm, a CO_2 percentage of 1 percent of the total dissolved gasses results in a partial CO_2 pressure of 2 atm. Although for some sites the total gas pressure could not be determined using the bubble point method (GPC, 2014), the partial CO_2 pressure can be estimated when assuming calcite equilibrium in the reservoirs (Figure 6). This suggests the highest partial CO_2 pressure for site 6 (WN) of around 3 to 4 atm. For the other sites, partial CO_2 pressures below 1.5 atm are estimated. This is similar to the range of partial CO_2 pressures estimated for hydrostatic pressures of over 200atm for the reservoir depths over 2km and the CO_2 gas fractions of 1 to 4% for the produced water at these sites (Figure 4).

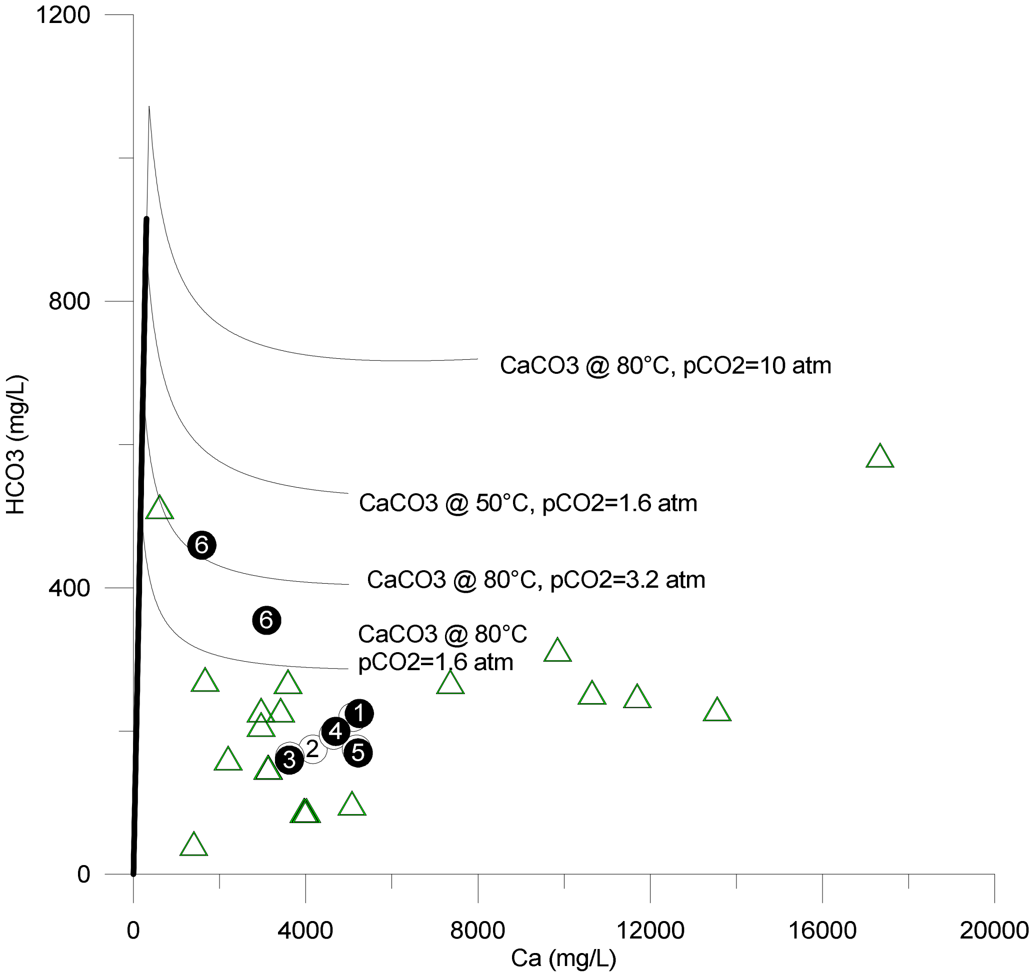

Figure 6: Calcium (Ca) and alkalinity (HCO3) concentrations for the sites studied. Numbers refer to the sites as listed in Table 1. Black circles refer to the compositions of the produced water, white circles refer to the composition of the injected water. Triangles indicate measurements in various Dutch reservoirs (Verweij, 2003). The lines are equilibrium scenarios for different partial CO2 pressures and temperatures as modelled using PHREEQC. The bold black line represents the stoichiometric ratio along which calcite would precipitate due to CO2 degassing.

3.1.4 Barite supersaturation

In addition to carbonate minerals, the precipitation of barite ($BaSO_4$) was identified as an additional potential scaling problem (Figure 7), with the highest potential observed for site 4 (DVS). However, modeling indicates that the solutions are 100 (SI=2) to 1000 (SI=3) times supersaturated with respect to the theoretical solubility product of barite, as are various Dutch reservoirs (Verweij, 2003). This indicates that barite precipitation is inhibited in these geothermal reservoirs, possibly because of brine composition. If the barite does not precipitate from the geothermal water in the reservoir at such high supersaturations, there is little reason to assume that barite would precipitate in the geothermal system after production, particularly as the temperature decline has only a limited effect on the degree of supersaturation.

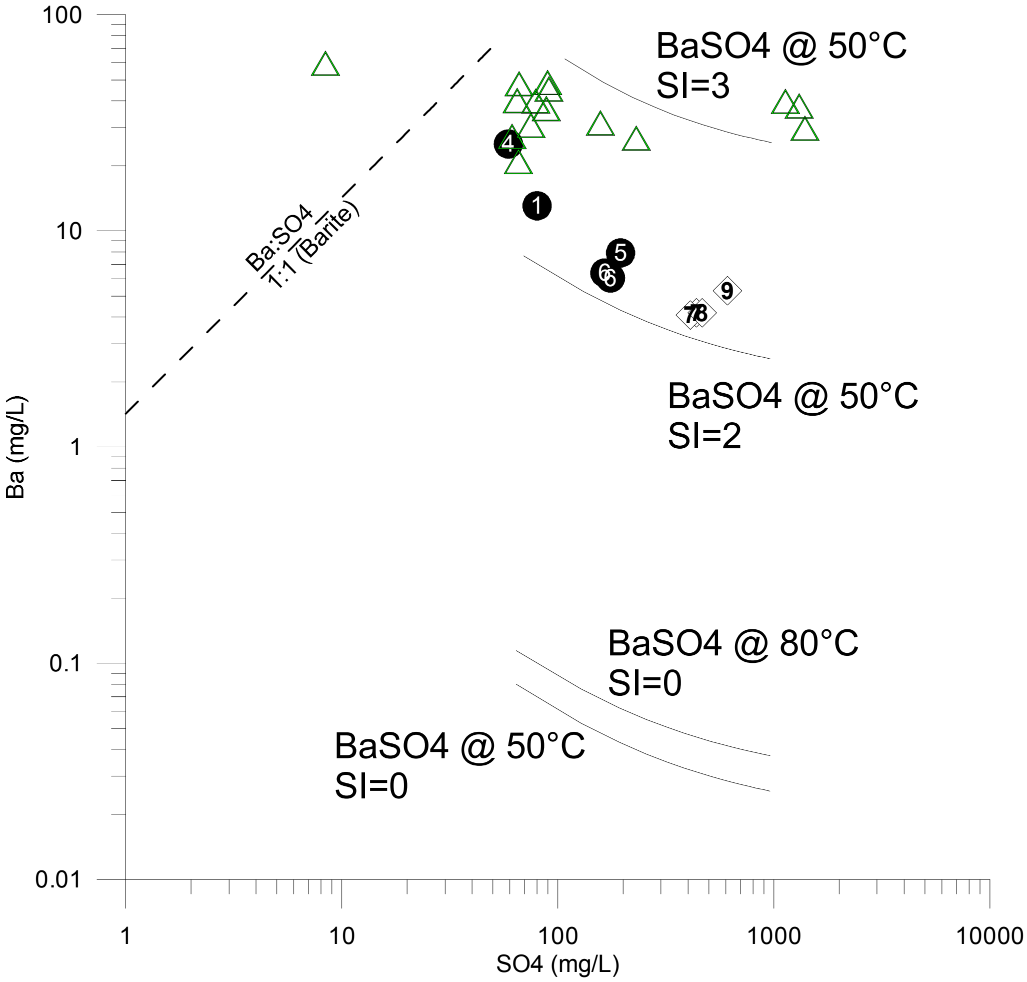

Figure 7: Barium (Ba) and sulphate (SO4) concentrations for the sites studied. Numbers refer to the sites as listed in Table 1. Black circles refer to the compositions in the produced water. Triangles indicate measurements in various Dutch reservoirs (Verweij, 2003). Diamonds indicate the compositions from the compilation by (Wasch, 2014). The lines are equilibrium scenarios for different temperatures and saturation indices (SI) as modelled using PHREEQC. The SI values represent the log value of the solubility product divided by the equilibrium constant. The dashed line represents the stoichiometric ratio along which barite would precipitate (or dissolve).

3.2 Scaling composition

In the four accumulations analysed, the most abundant elements (Table 5) are calcium for site 1 (AML), iron for site 5 (GW) and lead for site 7 (ACK). The lack of silicium or barium enrichments confirms the insignificance of silica or barite precipitation. Besides the absolute abundance, the relative increase of elements in the composition of the accumulates with respect to that of the produced water, indicates the preferential concentration of that element as would be expected for mineral precipitates. For all four accumulates analysed, lead and iron were concentrated with respect to calcium in comparison to their produced water composition by an average factor of 100,000 (Figure 8) and 50 (Figure 9) respectively. This is indicative of the preferential precipitation of the less soluble lead and iron carbonates relative to calcium carbonate (calcite).

Table 5: The 7 elements with highest content in the accumulations analyzed

Rank	**1 (AML) Scalant**		**1 (AML) Filter**		**5 (GW) Filter**		**7 (ACK) Scalant**	
	Element	wt. %	Element	wt. %	Element	wt. %	Element	wt. %
1	Ca	19,7	Ca	14,1	Fe	18,8	Pb	56,1
2	Fe	3,2	Fe	11,1	Cl	5,6	Cl	4,0
3	SO4	2,2	SO4	2,2	Na	3,4	Na	2,2
4	Cl	0,5	Cl	1,2	Mn	1,9	Ca	1,3
5	Mg	0,5	Na	0,7	SO4	1,7	Fe	0,9
6	Na	0,3	Mg	0,4	Ca	0,5	SO4	0,1
7	Sr	0,2	Mn	0,3	Pb	0,5	Mg	0,1

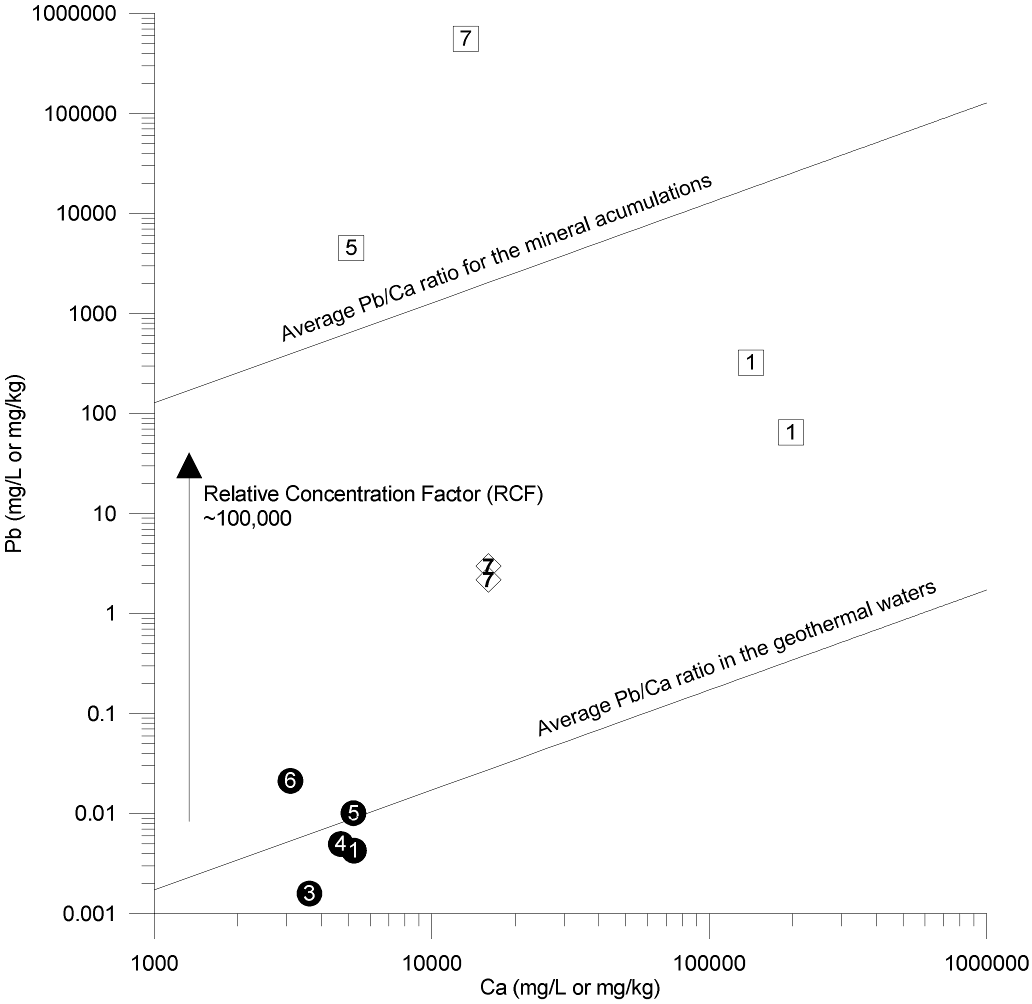

Figure 8: Calcium (Ca) and lead (Pb) concentrations the produced water and accumulates at the sites studied. Black circles refer to the compositions in the produced water in mg/L. Squares indicate the

concentrations in the accumulations in mg/kg. Numbers refer to the sites as listed in Table 1. Diamonds indicate the compositions of produced water from the compilation by (Wasch, 2014). The lines are the through-the-origin fits, representing the average Pb/Ca ratios for the produced water and accumulates.

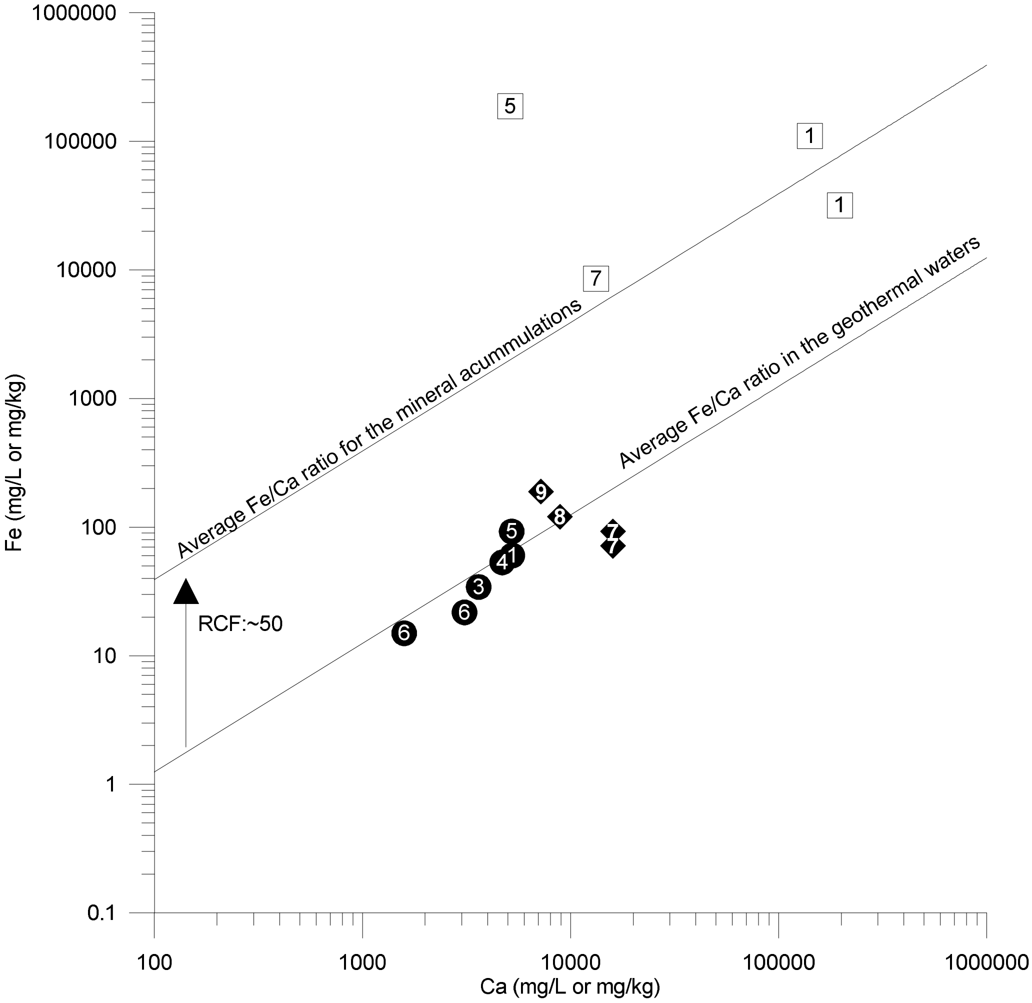

Figure 9: Calcium (Ca) and iron (Fe) concentrations of the produced water and accumulates at the sites studied. Black circles refer to the compositions in the produced water in mg/L. Squares indicate the concentrations in the accumulations in mg/kg. Numbers refer to the sites as listed in Table 1. Diamonds indicate the compositions of produced water from the compilation by (Wasch, 2014). The lines are the through-the-origin fits, representing the average Fe/Ca ratios for the produced water and accumulates.

The analysed accumulates were to various extents saturated with brine, which explains the relatively high chloride contents. Using the measured chloride concentration in the accumulates with the corresponding produced water composition allowed estimation of the residual brine water content (Table 6). Although this water content also fully explained the measured sodium concentrations, sulphate concentrations are enhanced relative to the concentrations based on brine water composition for the accumulates of site 1 (AML) and 5 (GW), indicating a minor contribution of sulphate precipitation. Overall, however, the precipitates appear to be dominated by the precipitation of carbonate phases, as was confirmed when conducting an acid test on the accumulates to verify the dissolution of the accumulate and the production of gas (CO2), following:

$CaCO3 + 2H^{+} = Ca^{2+} + CO_2(g) + H_2O$

While the observed effervescence was high (+) to very high (++) for the AML and ACK accumulates (Table 6), it was low (-) for the Fe-rich GW accumulate. This is in keeping with the known low dissolution rate of iron carbonates in acid (e.g. (Hartog, 2003)).

Table 6: Overall characterization of the accumulates analyzed

Site #	**Code**	**Type**	**Water %**	**Acid Test**	**Residue**		**Carbonate phase**	
					Present	Aceton solvable	Main	Minor
1	AML	Scalant	7.4	+	yes	yes	CaCO3	FeCO3
		Filter	17.3	+	yes	yes	CaCO3	FeCO3
5	GW	Filter	72,1	-	yes	yes	FeCO3	MnCO3
7	ACK	Scalant	35,2	++	no	-	PbCO3	CaCO3

The residual brine water content dilutes the elemental abundancies in the overall analysis of the accumulate composition largely with sodium and chloride (Table 5), particularly for the GW and ACK samples. The consideration of this residual brine water content (Table 6), indicates that the carbonate phases are indeed the main component of the accumulations studied. For site 1 (AML) the accumulations consists of mixture of mainly Ca-carbonate mixed with Fe-carbonate (Table 6), while for site 5 the carbonate phase is predominantly Fe-carbonate with probably minor contributions of Mn-carbonates. The carbonate precipitate from site 7 (ACK) largely consists of Pb-carbonate with only minute contributions by Ca and Fe. It is unlikely that metallic lead contributed to the total lead content, as there was no residue following the acid test. However, metallic lead is a known scaling from gas production facilities in the Schlochteren reservoir (Schmidt, 2000). The potential to form this scale results from the production of lead containing reservoir water. Rather than direct steel corrosion by dissolved lead, corrosion by the degassing induced precipitation of Pb-carbonate scaling might result at the steel-precipitate interface as follows:

$Fe^{0} + PbCO3 = FeCO3 + Pb^{0}$

Expectedly, this would result in elevated iron fractions in the carbonate phase, which were not observed (Table 5). Also, since no residue was detected after removing all carbonates with the acid test (Table 6), no significant amounts of metallic lead were present in the analysed accumulate from site 7 (ACK).

In contrast with the accumulate from site 7 (ACK), the accumulates from sites 1(AML) and 5(GW) did yield residues after dissolution of all carbonates with the acid test (Table 6). The residues represented less than a few percent of the initial accumulate mass. The fact that these residues did not dissolve in water or acid, but did readily dissolve in aceton, indicates that these residues are organic, probably oil-related, in nature. The exact nature and extent which these hydrophobic components might contribute to injectivity problems is not yet clear.

3.3 Waterquality changes to assess the formation of mineral precipitates

The comparison of produced and injected water compositions appears as a straightforward approach to addressing the geochemical processes that occur in the geothermal system. However, since the geothermal systems are operating with high flow rates (e.g. 100-200 m^3/hr) even very small compositional changes can result in the build-up of precipitates and injectivity problems. Therefore, reaction rates must be sufficiently high to be able to monitor quality differences between produced and injected water.

Particularly, for the process of degassing these rates appear to be very high. Degassing already occurred in the production wells (GPC, 2014) before the point where the production water could be sampled. Also observed in the production well is the presence of many small particles (GPC, 2014). These particles are likely carbonate particles that are formed as a result of the loss of CO2 pressure that occurs with degassing, as described in GPC (2014). To distinguish between dissolved and particulate solids, the commonly used, operationally defined exclusion size of 0.45 µm was used for filtration. Since a large fraction of the produced particles measured were smaller (GPC, 2014), a strict isolation of dissolved concentrations turned out to be impossible.

To test whether the extent to which the filtration of samples removed particles, all water samples were additionally analysed without filtration. Overall, the differences between the composition of filtered and unfiltered, and produced and injected water was very small. This can be explained when a large fraction of the particles formed during production and in the geothermal system were not separated by filtration. Small differences between filtered and unfiltered water were however observed for some elements (Figure 10). Filtration seems to impact calcium concentrations more than iron concentrations. This is however not conclusive, since this could either be the result of less Fe-carbonate particle formation or by a generally smaller particle for Fe-rich carbonate particles compared to Ca-rich carbonate particles. However, since the difference between filtered and unfiltered water is larger for the injection water, this suggests that iron-rich carbonate particles are formed later than the Fe-rich carbonate particles. Also, the largest difference in calcium concentrations for site 1 (AML) and the absence thereof for site 5 (GW), is in keeping with the relative importance of calcium carbonates in the analysed accumulations for these sites (Table 6).

-

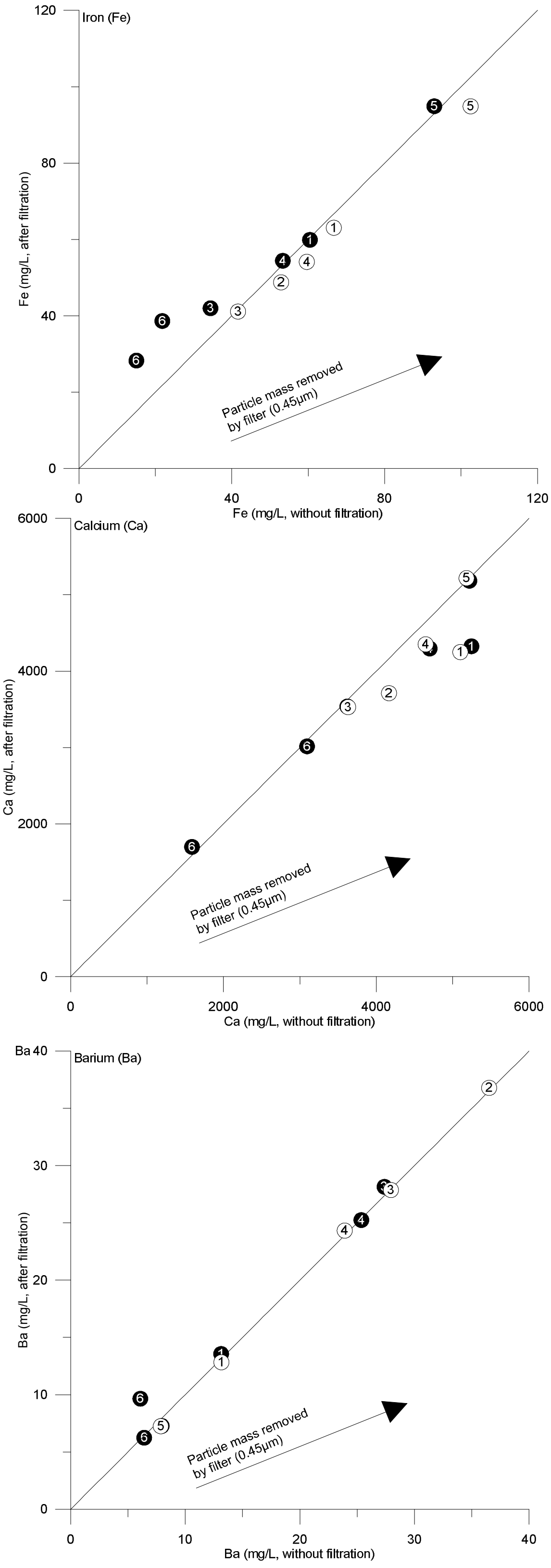

Figure 10: Comparsion of measured concentrations for iron, calcium and barium, with and without filtration over a 0.45 µm filter. Numbers refer to the sites as listed in Table 1. Black circles refer to the compositions in the produced water, white circles refer to the composition in the injected water.

3.4 A step-wise approach towards improving injectivity

Based on the geochemical analysis of the prodution waters and accumulations from several of the geothermal systems, carbonate precipitation due to degassing of CO2 appears to be the foremost factor causing scaling and injectivity problems. The cooling that occurs through the extraction of heat is not expected to increase the precipitation potential as most of the carbonates are more soluble at lower temperatures. Only where the precipitation of lead carbonate is dominant (such as for site 7, ACK), lower injection temperatures are likely to lead to additional precipitation.

Preventing degassing altogether is not a feasible strategy as it would require the surface installation to operate under the much higher pressures of the reservoir (e.g. >200atm for a reservoir depth at 2km). Therefore, the use of a degasser in a geothermal system aids in preventing the formation of free gas and potential gas clogging further on. However, since degassing of CO2 acts as the main driver for the carbonate precipitation observed, CO2 pressure control also provides the main key to its prevention. Luckily, CO2 appears to only represent a small fraction of the total gas pressure in the geothermal reservoirs studied (Figure 6). And in principle, it is only this partial CO2 pressure that would need to be maintained or restored to prevent or re-dissolve carbonate precipitation. For sites with lead carbonate precipitation, an increased CO2 pressure is required to compensate for the decrease of lead carbonate solubility with lower temperatures.

For the geothermal sites studied, the highest partial CO2 pressure is deduced for site 6 (WN) at 3-4 atm. This pressure is well below the typical operational pressure under which the surface part of geothermal systems is typically maintained (10-20atm). These operational pressures are therefore sufficiently high to allow the addition of sufficient CO2 to restore the partial CO2 pressure of the reservoir, while keeping all added CO2 dissolved throughout the system. For the re-dissolution of a carbonate mineral:

$$XCO_3(s) + CO_2(g) + H_2O(l) = X^{2+} + 2\ HCO3^-$$

Where X can be any divalent cation (Ca, Pb, Fe, Mn, Mg etc).

Based on this study, the following step-wise approach to improving injectivity for a geothermal site is proposed:

1. Establish how CO2 dosing would be best integrated, taking into account the various operational aspects (degasser, operational pressure, injection pressure and temperature)
2. Optimize CO2-dosing based on the site-specific partial CO2 pressure and type of carbonate precipitate, to prevent precipitating or enable re-dissolving the carbonate phase(s) again.
3. The use of hydrochloric acid dosing can be considered as a faster, more aggressive method to restore injectivity after which injection with CO2 dosing can maintain injectivity. Since acid treatment of carbonates results itself in CO2 production, care has to be taken not to generate CO2 quantities beyond the pressures maintained during operation.
4. The use of surfactants can be considered. These typically aid in keeping cations in solution, but are hard to target specifically the cations that are involved in the precipitation of carbonate phases. Therefore the use of this type of inhibitors requires significant overdosing. Also, the effectiveness of these inhibitors is likely

limited once particles have already precipitated in the system, e.g. in the production well. However, surfactant use seems to be suitable for target purposes, such as the prevention of scaling of the heat exchanger, for particular minerals that lower solubilities at lower temperatures.

5. Beyond the precipitation of carbonates, results indicate the formation of oil residues in scaling and on filters (Table 6). For now, it is uncertain to what extent these oil residues also contribute to some of the injectivity problems. This would require further study, which in part will become clear once the prevention of carbonate precipitation is appropriately addressed.

4 Conclusions

The causes of injectivity problems at several geothermal systems used by the greenhouse industry were investigated by analysing the geochemical aspects and processes involved. This study focuses on the causes of the poor injectivity due to the precipitation of minerals, as mineral scaling was suspected to be a major contributor to the injectivity problems.

It is concluded that the main cause for accumulation of minerals on filters and as scaling is due to the degassing of CO2 during the rise in the production well and in subsequent parts of the geothermal system. The CO2 degassing results from the drop in the gas pressure from reservoir depth (up to hydrostatic pressure) to the relatively low pressure at which the geothermal system at the surface is operated. The loss of CO2 results in subsequent precipitation of carbonate minerals.

Depending on the chemical composition of the geothermal water in the reservoir, Ca-rich, Fe-rich or Pb-rich carbonates were preferentially precipitated, as was confirmed by analysis of filter and scaling accumulates from various systems.

Since degassing of CO2 pressure acts as the main driver for the carbonate precipitation observed, CO2 pressure control also provides a solution. Since CO2 appears to only represent a relatively small fraction of the total gas pressure in the geothermal reservoirs studied, only a limited level of CO2-dosing is required to prevent or re-dissolve carbonate precipitates. The required partial CO2 pressure seems well achievable within the operational pressures currently maintained in the geothermal systems. Particularly the dosing of CO2 after degassing has potential as the use of a degasser allows the removal of other gasses (such as methane), increasing the gas pressure with which CO2 can be dosed. For sites with lead carbonate precipitation, an increased CO2 pressure is required to compensate for the decrease of lead carbonate solubility with lower temperatures.

5 References

GPC, 2014. Assessment of Injectivity Problems in Geothermal Greenhouse Heating Wells.

Hartog, N., 2003. Reactivity of Organic Matter and Other Reductants in Aquifer Sediments. Utrecht University.

Schmidt, A.P., 2000. Naturally Occurring Radioactive Materials in the Gas and Oil Industry: Origin, Transport and Deposition of Stable Lead and 210pb from Dutch Gas Reservoirs. Universiteit Utrecht.

Verweij, J.M., 2003. Fluid Flow Systems Analysis on Geological Timescales in Onshore and Offshore Netherlands: With Special Reference to the Broad Fourteens Basin. Netherlands Institute of Applied Geoscience TNO, National Geological Survey.

Wasch, L.J., 2014. Geothermal Energy – Scaling Potential with Cooling and Co2 Degassing. TNO 2013 R111661, TNO.